Catalysis Letters Vol. 103, Nos. 1–2, September 2005 (© 2005)
DOI: 10.1007/s10562-005-7522-2

In situ MRI study of 1-octene isomerisation and hydrogenation within a trickle-bed reactor

Andrew J. Sederman, Michael D. Mantle, Christopher P. Dunckley, Zhenyu Huang, and Lynn F. Gladden*

Department of Chemical Engineering, University of Cambridge, Pembroke Street, Cambridge CB2 3RA, United Kingdom

Received 12 July 2005; accepted 14 July 2005

^{13}C DEPT-MRI is used to provide the first spatial mapping of alkene isomerisation and hydrogenation during an alkene hydrogenation reaction occurring within a trickle-bed reactor. The implementation of a pulse sequence combining the spatial resolution of a magnetic resonance imaging (MRI) pulse sequence with a ^{13}C DEPT magnetic resonance spectroscopy pulse sequence enables spatially resolved ^{13}C spectra to be recorded of natural abundance ^{13}C species. Observation of the ^{13}C nucleus, which has a much larger chemical shift range than the ^{1}H nucleus, provides spectra from which direct identification of the products of isomerisation and hydrogenation is achieved. This technique is illustrated with respect to the hydrogenation of 1-octene over a 1 wt% Pd/Al_2O_3 catalyst. In this preliminary study we demonstrate the ability of this technique to identify the effect of changing the hydrogen flow rate on the evolution of isomerisation and hydrogenation processes occurring along the length of the bed.

KEY WORDS: DEPT MRI; trickle-bed reactor; hydrogenation; magnetic resonance imaging.

1. Introduction

It has long been appreciated that the performance of a heterogeneous catalyst developed at the bench scale, in terms of both activity and selectivity, may be substantially decreased when that catalyst is formed into larger pellets and then packed into a heterogeneous catalytic reactor such as a fixed bed. It therefore follows that the catalyst and reactor need to be designed as an integral unit, ideally this design being based on a rigorous understanding of the mass transfer and chemical processes occurring within the reactor. Unfortunately the necessary understanding of the coupling of mass transfer, heat transfer and chemical kinetics remains weak because of a lack of non-invasive spatially resolved measurement techniques able to probe optically opaque chemical reactor environments. However, it is in this application that magnetic resonance (MR) imaging techniques offer significant potential. MR flow imaging has already revealed the high degree of flow heterogeneity within fixed-bed reactors; in some regions of the inter-particle space, fluid velocities may be an order of magnitude faster than in other regions of the bed [1]. Under such circumstances the contact time between the feed and catalyst, as well as the mass (and heat) transfer to and from the catalyst pellets will vary within the bed; such spatial variation in hydrodynamics and mass transfer is expected to cause spatial variations in the activity and selectivity within the bed. However, very few experiments have so far been reported to address and, more importantly, quantify these phenomena. In this paper we report the first application of a spatially resolved measurement of chemical composition within a trickle-bed reactor using natural abundance ^{13}C MRI. This development is significant because the ability to employ ^{13}C as opposed to ^{1}H observation provides a generic tool that can be used to study a wide range of heterogeneous catalytic reactions. Further, the ability to observe natural abundance ^{13}C, as opposed to requiring isotopically enriched reactants means that it is not prohibitively expensive to study continuous processes using this approach. In this study we use ^{13}C Distortionless Enhancement by Polarization Transfer (DEPT) MRI to study octane hydrogenation *in situ* within a laboratory-scale trickle-bed reactor. In this reactor, the fixed bed of catalyst pellets is contacted by a gas-liquid two-phase flow and is operated under conditions of co-current downflow. This trickle-bed reactor configuration is typical of that used widely in the petroleum, petrochemical and chemical industries, as well as finding increasing applications in biochemical and electrochemical processing and waste treatment. Typical reactions carried out in trickle-bed reactors involve hydrogenations, oxidations and various types of hydrotreatments, e.g. hydrocracking, hydrodenitrogenation and hydrodesulphurisation.

MR techniques in catalysis are well established but have focussed predominantly on NMR spectroscopy studies of catalyst characterisation and *in situ* studies of reaction, most often performed on the catalyst in powder form [2,3]. To a lesser extent measurements of molecular diffusion [4–7], liquid distribution during reaction [8] and coke distribution [9–11] within both single catalyst pellets and arrays of such pellets have been addressed. These studies have used both spatially unresolved and microi-

*To whom correspondence should be addressed.

maging MR methods. It is only recently that MR techniques have been applied to study chemical composition during reaction within arrays of catalyst pellets. To date, three different approaches have been reported. The first two of these used ^{1}H MRI chemical mapping techniques. Whilst successful in developing this field of research, both illustrate the limitations of using ^{1}H observation as a generic approach. To stress the limitations of using ^{1}H observation may appear counter-intuitive. Successful spatial resolution of a spectroscopic measurement requires sufficient signal-to-noise to be achieved within small volume elements within the macroscopic sample. This would suggest that ^{1}H observation is the technique of choice, thereby exploiting the 99.9% natural abundance and inherent NMR sensitivity of the ^{1}H nucleus. However, the disadvantage of using ^{1}H observation is that the ^{1}H nucleus has a relatively narrow chemical shift range which, combined with the large number of ^{1}H resonances present in a typical spectrum of a hydrocarbon reaction and the broadening of these resonances as a result of decreased spin–spin relaxation times arising from the large liquid–solid interfacial area within the sample, gives rise to a large number of overlapping resonances making spectral assignment and the quantification of peak intensities difficult. In the first report of chemical mapping within a fixed bed, Yuen *et al.* [12] used volume selective magnetic resonance spectroscopy to quantify the conversion of an esterification reaction occurring within a fixed bed of ion exchange resin. Conversion was quantified by the chemical shift of the ^{1}H resonance of the OH groups present in the reaction mixture within the interparticle space of the bed. This approach can only be used for reactions in which the ^{1}H spectrum is relatively simple such that assignment of changes in chemical shift can be related unambiguously to changes in chemical conversion. More recently, Koptyug *et al.* [13] used ^{1}H NMR to produce spatially resolved spectra within a 2-D slice section along the axial direction of a fixed bed of 1 wt% Pd/Al_2O_3 catalyst pellets. The reaction considered was that of the hydrogenation of α-methylstyrene to cumene. The spectra show evidence of changes in chemical composition along the length of the bed, but conversion was not quantified – most likely due to problems in deconvolving the ^{1}H resonances associated with the reactant and product species. The third, and most recent approach, was the implementation of a ^{13}C DEPT-MRI pulse sequence which was demonstrated in application to the competitive etherification and hydration reactions of 2-methyl-2-butene occurring within a fixed bed of H^+-ion exchange resin [14]. By moving to ^{13}C observation, spectral assignment is easier because the ^{13}C nucleus has a much wider chemical shift range than ^{1}H, thereby reducing the number of overlapping peaks. Consequently, individual spectral peaks are more readily resolved. However, given that the natural abundance of the ^{13}C nucleus is only 1.07% and its NMR sensitivity is lower than that of ^{1}H by a factor of 5870, there is considerable loss of signal-to-noise when employing ^{13}C as opposed to ^{1}H observation. In solid state NMR, which typically uses small, closed, sample volumes ($\sim$1 cm^3), this decrease in sensitivity and natural abundance is addressed by isotopically enriching the species of interest with ^{13}C. However, in studying chemical composition within a reactor operating under conditions of continuous flow, this approach is prohibitively expensive. In the present work, we implement the ^{13}C DEPT-MRI pulse sequence for the *in situ* study of isomerisation and hydrogenation of 1-octene in a trickle-bed reactor. The ^{13}C DEPT pulse sequence observes natural abundance ^{13}C by transferring polarisation from the ^{1}H to the ^{13}C nuclei, thereby providing enhancement of the ^{13}C signal. Further signal enhancement is achieved relative to a standard ^{13}C pulse-acquire experiment because many more signal averages can be acquired in a given period of time. This is because in the DEPT experiment the recycle time is determined by the spin-lattice relaxation time (T_1) of the ^{1}H nuclei and not the ^{13}C nuclei; for the system studied here $T_1(^{13}C) \asymp 3-5\ T_1(^{1}H)$. In this study of the hydrogenation of 1-octene, we show that the data obtained, even without detailed analysis, provide a characterisation of the product selectivity as a function of position along the length of the reactor. A more detailed analysis of the spectra is then reported to quantify the product distribution. In particular we consider the effect of hydrogen flow rate on the extent of isomerisation and hydrogenation occurring along the length of the bed.

1-Octene hydrogenation was selected as the reaction for study because it occurred rapidly under conditions of low temperature and pressure such that a significant amount of isomerisation and hydrogenation occurred during a single pass over a $\sim$3 cm length of the fixed bed; this length scale being the maximum dimension of the field-of-view in the imaging experiment. Reaction occurring over length scales greater than this can be followed by adjusting the position of the reactor within the superconducting magnet employed in the MRI experiment. The selective hydrogenation of unsaturated hydrocarbons is of importance in various processes within refining, polymerisation and fine chemicals industries to generate primary products or high value intermediates, and to prevent poisoning of catalysts [15,16]. Studies of 1-octene hydrogenation have been reported for various reactor types including slurry, monolith and trickle bed configurations [17–20]. From these studies it is clear that the selectivity of the reaction is significantly influenced by the reactor type and operating conditions employed.

2. Experimental

2.1. Experimental setup

1 wt% Pd/Al_2O_3 catalyst (Johnson Matthey plc) was loaded to a height of 3 cm in a glass reactor of inner diameter 2.5 cm. The catalyst was in the form of trilobes

of diameter 1.0 mm and length 6 ± 2 mm, and had a BET surface area and pore volume of 97.6 $m^2\ g^{-1}$ and 0.49 $cm^3\ g^{-1}$, respectively. Above the catalyst, pure Al_2O_3 trilobes, from the same batch as those used in the preparation of the catalyst, were loaded to a height of 3 cm to increase saturation of the liquid feed with H_2 before contact with the catalyst as well to enhance liquid distribution across the bed. Pure Al_2O_3 trilobes had also been loaded into the bottom of the reactor prior to loading the Pt/Al_2O_3 catalyst. The reactor was then inserted into the MR probe within the superconducting magnet. Air at room temperature was passed through the bore of the magnet during the experiment to remove heat generated by the hydrogenation reaction.

The Pd/Al_2O_3 catalyst was reduced *in situ* within the reactor using 20% H_2 in N_2 fed at a rate of 1200 mL min^{-1} for 2 h. 1-octene (98%, Aldrich) was then pumped into the reactor using a positive displacement HPLC pump (Pharmacia, P-6000) for a period of 45 min to fully wet the catalyst surface. A 3-D MR image was acquired to confirm that the bed was uniformly wet throughout. After this, both gas and liquid were then passed into the reactor at flow rates of 32 and 1.0 mL min^{-1}, respectively. The ^{13}C DEPT-MRI experiments were performed at time intervals of 17 min until steady state was achieved; i.e. successive data acquisitions showed negligible differences between spectra acquired at a given axial location within the bed. A second experiment was then performed on the same catalyst packing, again operating at steady state, but with a higher gas flow rate of 64 mL min^{-1}.

2.2. MRI

Imaging of conversion within the fixed bed was achieved using a proton-decoupled ^{13}C DEPT spectroscopy pulse sequence [21] integrated into an imaging sequence [22]. A schematic of the ^{13}C DEPT-MRI pulse sequence used is shown in figure 1. All ^{13}C DEPT-MRI experiments were performed using a Bruker Biospin DMX-200 NMR spectrometer with a 4.7 T vertical magnet, equipped with shielded gradient coils providing a maximum gradient strength of 20 G cm^{-1}. A Bruker mini 0.5 probe equipped with a birdcage r.f. coil of diameter 38 mm was used, dual-tuned to 199.70 and 50.22 MHz for the ^1H and ^{13}C resonances, respectively. The duration of both the ^1H and ^{13}C 90° pulses was 75 μs. The phase encoding gradient was of duration 0.5 ms and was ramped to a maximum value of 3.13 G cm^{-1} in 16 increments. The field-of-view in the axial (z) direction was 45 mm giving a spatial resolution in the axial direction of 2.81 mm. In summary, 16 spectra are recorded along the length of the bed. The spectra are acquired from volume elements of side length 2.81 mm in the z-direction, the data being averaged in the x–y plane. The location at which the spectra were acquired along the length of the bed is identified as the mid-point of each volume element in the axial direction. The position of the interface between the pure alumina and catalyst packings at the top of the bed is identified as $z = 0$ mm. Increasing z-values indicate the direction of superficial flow. When acquiring the MR data it is important that the olefinic and aliphatic regions are acquired separately since the DEPT enhancement is only efficient when the r.f. irradiation of both ^1H and ^{13}C nuclei are on or close to resonance. 16 averages were acquired for each spectral region with a recycle delay of 2 s yielding a total acquisition time of 17 min for the complete datasets of both the olefinic and aliphatic regions.

Product selectivity along the length of the trickle-bed reactor is determined by using the following spectral assignments given in table 1. All chemical shifts are reported relative to the ^{13}C resonance in tetramethylsilane (TMS). A qualitative analysis of the selectivity of the reaction is obtained on the basis of these assignments. To perform a quantitative analysis it is important to recognize that unlike in a single pulse-acquire sequence, for which the intensity of the signal is proportional to the number of nuclei present in the sample, in the DEPT experiment the ^{13}C signal intensity, I, is described by equation (1):

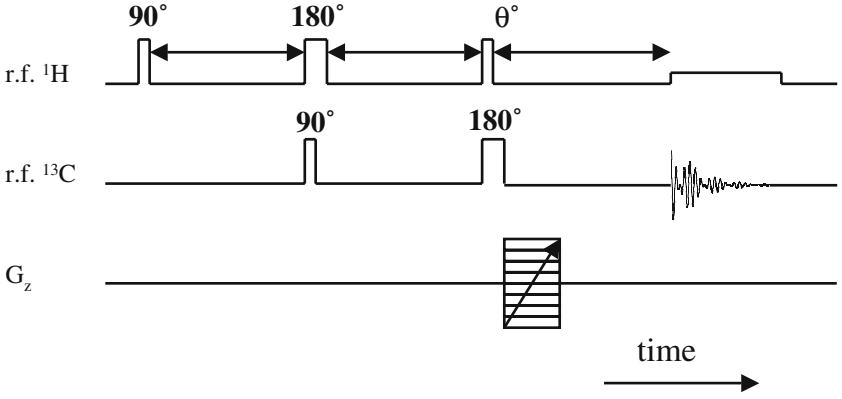

Figure 1. ^{13}C DEPT-MRI pulse sequence. The signal is acquired under conditions of ^1H decoupling.

Table 1
Chemical shifts of the olefinic and aliphatic ^{13}C resonances of 1-octene, *n*-octane and 2-,3- and 4-octene isomers

	Olefinic ^{13}C resonances	Aliphatic ^{13}C resonances
n-octane	–	14.16; 22.88; 29.54; 32.15
1-Octene	114.12; 139.25	14.11; 22.75; 28.97; 29.06; 31.89; 33.94
cis-2-Octene	123.68; 131.05	12.75; 14.15; 22.8; 27.02; 29.5; 31.76
trans-2-Octene	124.61; 131.82	14.11; 17.91; 22.75; 29.52; 31.62; 32.77
cis-3-Octene	129.44; 131.65	14.06; 14.46; 20.69;22.52; 27.01; 32.24
trans-3-Octene	129.5; 132.04	14.04; 22.39; 25.79; 32.09; 32.46
cis-4-Octene	129.95	13.83; 23.08; 29.5
trans-4-Octene	130.47	13.69; 22.95; 34.94

Data are taken from the SDBS spectral database (http://www.aist.go.jp/RIODB/SDBS/cgi-bin/cre_index.cgi). All chemical shifts are referenced to TMS.

$$I(CH_n) = n \sin\theta \cos^{n-1}\theta \quad (1)$$

where H and C represent hydrogen and carbon nuclei and n represents the number of H nuclei bonded to the C nucleus of interest. θ is the tip angle of the final applied ^1H pulse in the DEPT sequence. For $\theta = 45^{\circ}$, as is used in this study, signal intensity from CH, CH_2 and CH_3 groups is acquired in the ratio 0.707:1.00:1.06. Two further influences on the quantitative nature of the data obtained have also been taken into account. First, it was confirmed that the spin–spin relaxation time (T_2) of all CH_n resonances was sufficiently long that relaxation contrast effects did not influence different CH_n resonances to different extents. It was found that the T_2 values of all CH_n species exceeded 100 ms, these values being significantly longer than the echo time of 6 ms used in the pulse sequence. Second, a correction to the spectral intensities was applied to account for the effect of any inhomogeneous response of the r.f. coil (commonly referred to as correcting for B_1 inhomogeneity). A 2-D DEPT-MRI reference image of the bed fully saturated with 1-octene was used to obtain the correction factor at each axial location; if the B_1 field is homogenous, the intensity of the spectral resonances at each axial position would be the same.

During the course of the reaction a ^1H image of the bed was acquired using the RARE pulse sequence [23]. The pulse sequence was implemented using a RARE factor of 16 (i.e. acquiring 16 lines of **k**-space from a single r.f. excitation) and an effective echo time of 25.6 ms. The total data acquisition time was 4 s. The 2-D image was taken with a field-of-view of 60 mm (z) × 30 mm (x) and a data array size of 128 × 64 points, thereby giving an isotropic in-plane spatial resolution of 468 μm. The image slice thickness was 2 mm. These images allow us to monitor the macroscopic liquid distribution within the bed during reaction.

3. Results and discussion

Figure 2 shows a typical spectrum recorded using spatially unresolved ^{13}C DEPT NMR spectroscopy; the spectrum is acquired over the whole catalyst bed. The spectrum was acquired with the bed operating at steady state for gas and 1-octene flow rates of 32 and 1.0 ml min^{-1}, respectively. As seen in table 1, the peaks occurring in the range in the range 10–40 ppm are associated with ^{13}C resonances in aliphatic environments, whereas resonances in the range 110–140 ppm are associated with olefinic ^{13}C species. It is important to note that the spectral assignments available from the database are obtained from pure liquid spectra. The spectra obtained in the present study are characterized by much wider line widths, arising from shorter transverse relaxation times (T_2^*) associated with

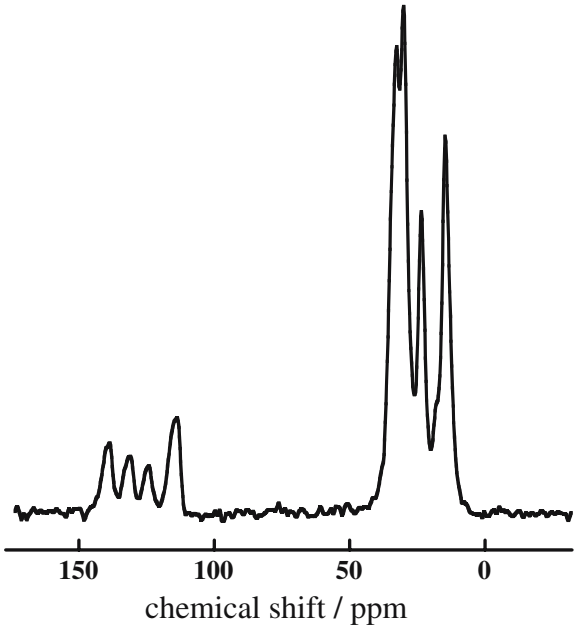

Figure 2. ^{13}C DEPT NMR spectrum recorded during the hydrogenation of 1-octene. Assignments are given in table 1. The peaks occurring at ~114 and ~139 ppm are associated with 1-octene. Additional resonances in the olefinic region of the spectrum are also seen at ~124 and ~131 ppm, these are a clear indication that 2-octene has been formed during reaction. The spectrum was acquired with the bed operating at steady state for gas and 1-octene flow rates of 32 and 1.0 mL min^{-1}, respectively. The spectrum shown has been obtained by merging separate ^{13}C DEPT acquisitions for each of the olefinic and aliphatic regions.

magnetic susceptibility variations within the system. Given these line-broadening effects, the chemical shifts observed in the spectra reported have an error of ± 1 ppm. Considering figure 2 and the data in table 1, it is seen that unambiguous assignments of spectral peaks to specific reactants, intermediates and products will be difficult in the aliphatic region due to multiple overlapping resonances. However, the olefinic region is much easier to interpret. In summary, we base our analysis on the following assignments: (i) 1-octene is clearly identified with resonances at ~114 and ~139 ppm; note the relative intensity of the $H_2C{=}^{*}CH{-}$ peak at ~139 ppm relative to that of the $H_2^{*}C{=}CH$ peak at ~114 is 0.7 (figure 2) which is due to the differing polarization transfer efficiencies of the CH and CH_2 environments as predicted by equation (1); here we use '*' to identify the C resonance of interest. (ii) The peak at ~124 ppm (associated with CH moieties) is due solely to *cis*-2 and *trans*-2-octene whereas the peak at ~131 ppm is a superposition of all isomers of 2-, 3- and 4-octenes. Therefore, subtraction of the integral of the peak at ~124 ppm from that at ~131 ppm yields the amount of 3- and 4-octene isomers. Inspection of figure 2 shows that the dominant isomer is 2-octene because the intensities of the two peaks at ~124 and ~131 ppm are similar, although the slightly greater intensity of the peak at 131 ppm confirms that some 3- and may be 4-octene isomers are present.

Spatially resolved ^{13}C DEPT-MRI data are shown in figures 3–6. Figures 3 and 4 show data recorded at the same operating conditions as reported for figure 2. Figure 3a,b shows 2-D maps of ^{13}C DEPT spectra, spatially resolved along the length of the column. Any horizontal cut through the 2-D maps recovers a 1-D ^{13}C DEPT NMR spectrum, as shown below each map. The two solid horizontal lines indicate the limits of the catalyst packing within the bed. Figure 3c shows a ^{1}H image of liquid distribution within the bed. ^{1}H signal from all liquid species present is recorded; higher liquid contents are identified by lighter shades. Qualitative interpretation of the data shown in figure 3a confirms that above the catalyst only 1-octene exists within the bed, identified by peaks occurring at ~114 and ~139 ppm. As soon as the 1-octene feed reaches the catalyst, additional peaks in the spectrum are observed

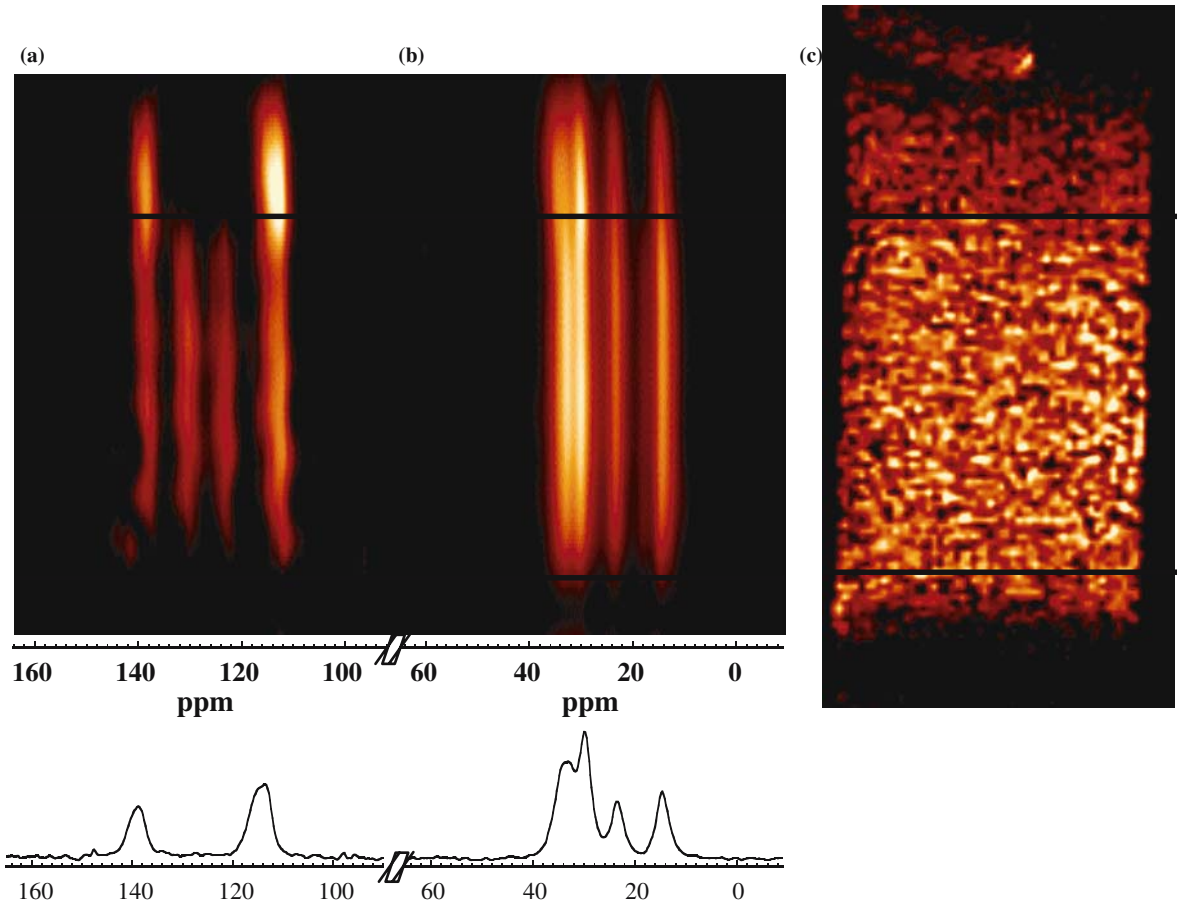

Figure 3. 2-D map of ^{13}C DEPT-MRI spectra recorded along the length of the trickle bed. Separate acquisitions were made for each of the (a) olefinic and (b) aliphatic regions of the spectrum. The data were acquired with the bed operating at steady state for gas and 1-octene flow rates of 32 and 1.0 mL min^{-1}, respectively. Below each 2-D map, the 1-D ^{13}C DEPT NMR spectrum recorded at the interface between the catalyst and pure Al_2O_3 packing is shown; the centre of this image voxel occurs at $z = -0.6$ mm. (c) 2-D ^{1}H MR image of the spatial distribution of liquid within the bed. The white, horizontal lines indicate the limits of the catalyst packing.

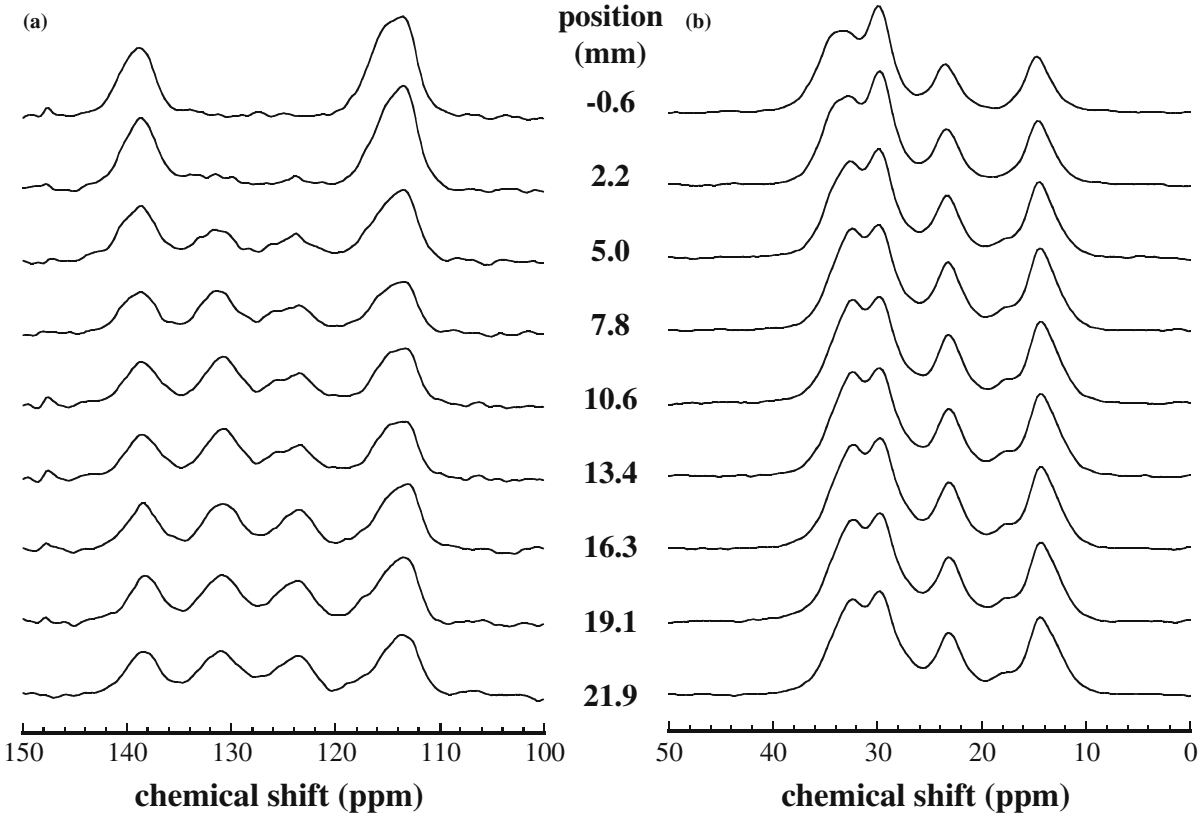

Figure 4. Spectra recorded at 9 positions down the bed for gas and liquid flow rates of 32 and 1.0 mL min^{-1}, respectively. Spectra are shown for (a) the olefinic region, and (b) the aliphatic region of the ^{13}C DEPT spectrum.

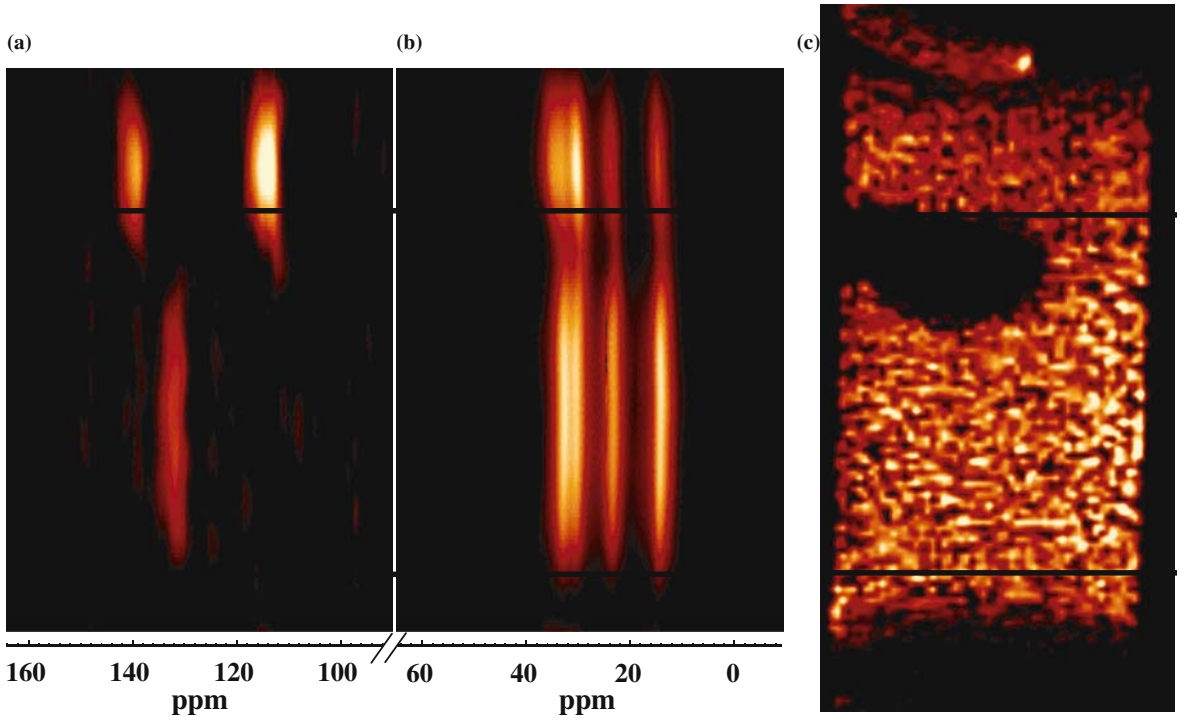

Figure 5. 2-D map of ^{13}C DEPT-MRI spectra recorded along the length of the trickle bed. Separate acquisitions were made for each of the (a) olefinic and (b) aliphatic regions of the spectrum. The data were acquired with the bed operating at steady state for gas and 1-octene flow rates of 64 and 1.0 mL min^{-1}, respectively. (c) 2-D ^{1}H MR image of the spatial distribution of liquid within the bed. At this higher gas flow rate greater reaction foccurs as the reactants contact the catalyst resulting in local vaporization within the bed identified by the region of zero signal intensity.

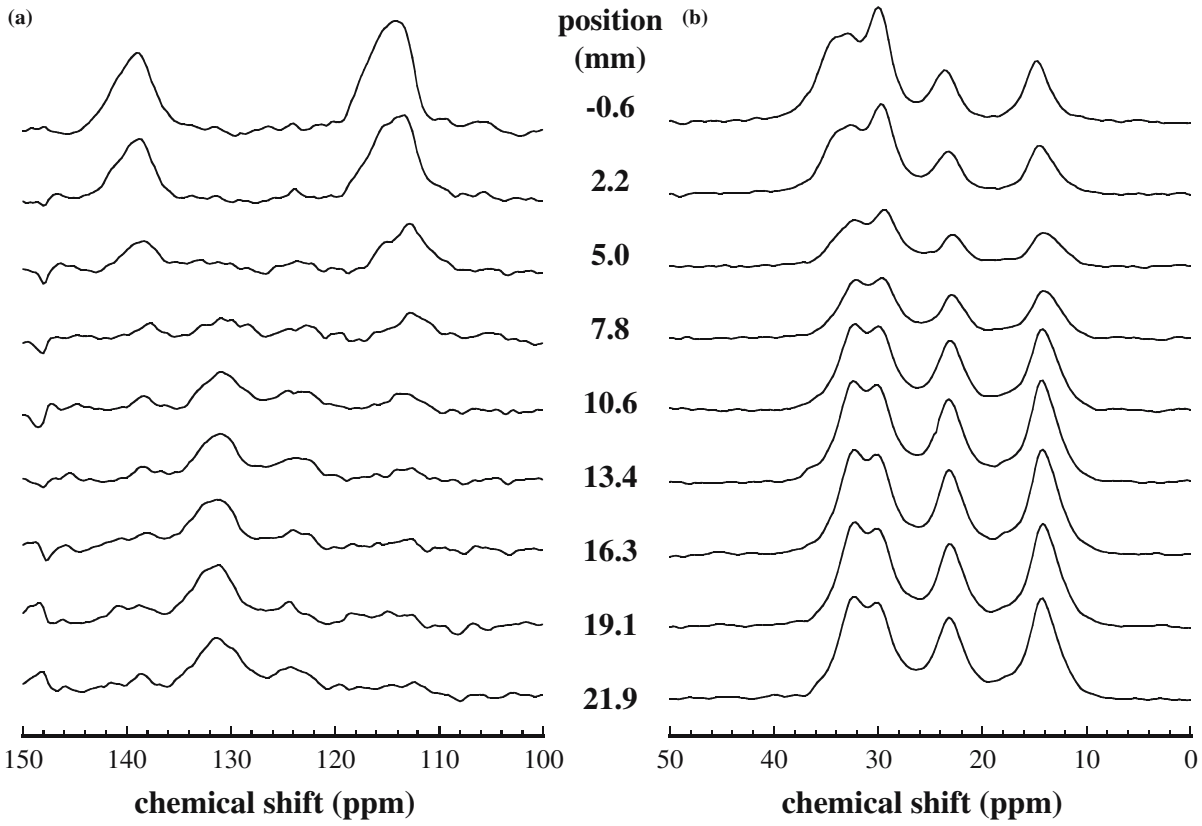

Figure 6. Spectra recorded at 9 positions down the bed for gas and liquid flow rates of 64 and 1.0 ml min^{-1}, respectively. Spectra are shown for (a) the olefinic region, and (b) the aliphatic region of the ^{13}C DEPT spectrum.

at ~124 and ~131 ppm indicating the formation of predominantly 2-octene isomers. The total integrated intensity of the spectral features in the olefinic region decreases confirming that some hydrogenation through to octane has occurred along the length of the bed. Figure 4 shows spectra extracted from the 2-D dataset at 9 positions down the bed. These spectra allow us to identify more clearly the species present within the column. The spectra from the olefinic region confirm the conclusions drawn from figure 3a; namely significant production of 2-octene isomers; there is also evidence of 3- and 4-octene isomers being formed due to the greater intensity of the peak at ~131 ppm relative to that at ~124 ppm. The aliphatic region (figure 4b) also shows that (i) there is a loss of spectral intensity at ~34 ppm consistent with loss of 1-octene; (ii) the appearance of a peak at 18 ppm confirming the formation of *trans*-2-octene; (iii) relatively little 3- and 4-octenes are formed since no detectable spectral intensity is observed at ~129 ppm.

Figures 5 and 6 show similar data recorded for a higher gas flow rate of 64 mL min^{-1} at the same 1-octene flow rate of 1.0 mL min^{-1}. Comparing figures 3 and 5 it is clear that increasing the gas flow rate has significantly influenced the product distribution. Figure 5c shows a loss of ^{1}H signal intensity immediately the feed encounters the catalyst. The extent of reaction is sufficient at this point to cause local vaporization of liquids, which results in loss of signal intensity and has been reported by earlier workers for the case of α-methylstyrene hydrogenation [13]. Under the acquisition conditions used here, gas phase species will not be imaged. This decrease in signal intensity is also seen in the 2-D ^{13}C DEPT-MRI spectra shown in figure 5a, b. As seen from figure5a, b to figure 6, as reaction progresses along the length of the reactor there is almost complete loss of spectral intensity at ~114 and ~139 ppm indicating the disappearance of 1-octene. As 1-octene is used up, so the intensity of a resonance at ~132 ppm increases. This feature is predominantly associated with *cis*- and *trans*- 3- and 4-octene, since the resonance at ~124 ppm, which is associated with 2-octene isomers, is of significantly lower intensity than that at ~132 ppm. It is also seen that the integrated intensity of the olefinic region decreases down the reactor while that of the aliphatic region increases, consistent with octane formation. Lack of any peak appearing at a chemical shift of ~35 ppm shows that significant amounts of trans 4-octene are not being produced suggesting that most of the further isomerisation from 2-octene is to 3-octene and not 4-octene.

Figure 7 shows the conversion and selectivity data for the reactor operating under low and high gas flow rate conditions, after correction for the effect of B_1 inho-

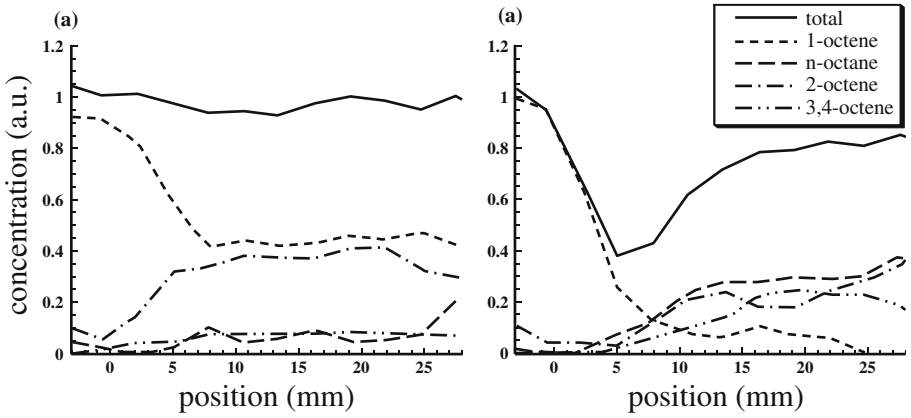

Figure 7. Concentrations of 1-octene, *n*-octane and the isomerisation products (2-, 3- and 4-octenes) are shown as a function of position along the bed for a gas flow rate of (a) 32 and (b) 64 mL min^{-1}. Concentrations are accurate to ± 0.05 arbitrary units.

mogeneity. In figure 7a, the data for the low gas feed rate are shown. It is seen that the total liquid concentration (i.e. the number of ^{13}C species in the liquid phase) remains approximately constant throughout the reactor. The concentration of 1-octene drops sharply to ~40% of the initial concentration at a distance of ~8 mm into the catalyst bed with the products at this location being principally 2-octenes. In figure 7b the significant decrease in the total concentration of species present at a position of ~5 mm down the reactor is associated with the vaporization event observed in figure 5c. At a distance 25 mm into the catalyst bed, there is no longer any 1-octene present within the bed, and the product distribution (3-, 4-octenes):2-octenes:*n*-octane is in the ratio 1:1.3:1.4 .

4. Conclusions

This work clearly demonstrates the ability of ^{13}C DEPT MRI to spatially resolve chemical conversion and selectivity during the hydrogenation of 1-octene within a trickle-bed reactor. In particular, we demonstrate that this 'chemical mapping' can be achieved with natural abundance ^{13}C using a NMR technique that can be applied to a wide range of heterogeneous catalytic reactions. Current studies are extending these studies to 2-D maps of chemical composition within the bed and exploring the effect of hydrodynamic parameters describing the bed on the conversion and selectivity characteristics observed.

Acknowledgements

We gratefully acknowledge EPSRC, Johnson Matthey plc and Robinson Brothers plc for financial support of this work. We also wish to thank S.D. Jackson and the University of Glasgow for providing the catalyst characterisation data.

References

[1] A.J. Sederman, M.L. Johns, P. Alexander and L.F. Gladden, Chem. Eng. Sci. 53 (1998) 2117.
[2] K.J. Packer, Top. Catal. 3 (1996) 249.
[3] J.F. Haw, Top. Catal. 8 (1999) 81.
[4] M.P. Hollewand and L.F. Gladden, Chem. Eng. Sci. 50 (1995) 309.
[5] M.P. Hollewand and L.F. Gladden, Chem. Eng. Sci. 50 (1995) 327.
[6] I.V. Koptyug, V.B. Fenelonov, L.Y. Khitrina, R.Z. Sagdeev and V.N. Parmon, J. Phys. Chem. B 102 (1998) 3090.
[7] I.V. Koptyug, L.Y. Khitrina, Y.I. Arsitov, M.M. Tokarev, K.T. Iskakov, V.N. Parmon and R.Z. Sagdeev, J. Phys. Chem. B 104 (2000) 1695.
[8] I.V. Koptyug, A.V. Kulikov, A.A. Lysova, V.A. Kirillov, V.N. Parmon and R.Z. Sagdeev, J. Am. Chem. Soc. 124 (2002) 9684.
[9] K.Y. Cheah, P. Chiaranussati, M.P. Hollewand and L.F. Gladden, Appl. Catal. A 115 (1994) 147.
[10] J.-L. Bonardet, T. Domeniconi, P. N'Gokoli-Kékélé, M.-A. Spinguel-Huet and J. Fraissard, Langmuir 15 (1999) 5836.
[11] N.-K. Bar, F. Bauer, D.M. Ruthven and B. Balcom, J. Catal. 208 (2002) 224.
[12] E.H.L. Yuen, A.J. Sederman and L.F. Gladden, Appl. Catal. A 232 (2002) 29.
[13] I.V. Koptyug, A.A. Lysova, A.V. Kulikov, V.A. Kirilov, V.N. Parmon and R.Z. Sagdeev, Appl. Catal. A 267 (2004) 143.
[14] B.S. Akpa, M.D. Mantle, A.J. Sederman and L.F. Gladden, Chem. Commun. (2005) 2741.
[15] A. Molnar, A. Sarkany and M. Varga, J. Mol. Catal. A 173 (2001) 185.
[16] T.A. Nijhuis, F.M. Dautzenberg and J.A. Moulijn, Chem. Eng. Sci. 58 (2003) 1113.
[17] M. Bartok, G. Szollosi, A. Mastalir and I. Dekany, J. Mol. Catal. A 139 (1999) 227.
[18] C. Liu, Y. Xu, S. Liao and D. Yu, J. Mol. Catal. A 149 (1999) 119.
[19] H.A. Smits, A. Stankiewicz, W. Glasz, T.H.A. Fogl and J.A. Moulijn, Chem. Eng. Sci. 51 (1996) 3019.
[20] B. Battsengel, L. Datsevich and A. Jess, Chem. Eng. Technol. 25 (2002) 621.
[21] M.R. Bendall, D.M. Doddrell and D.T. Pegg, J. Am. Chem. Soc. 103 (1981) 4603.
[22] H.N. Yeung and S.D. Swanson, J. Magn. Reson. 83 (1989) 183.
[23] J. Hennig, A. Nauerth and H. Friedburg, Magn. Reson. Med. 3 (1986) 823.